Analysis of Aerodynamically Induced Whirling Forces in Axial Flow Compressors

Proceedings of
ASME TURBOEXPO 2000
May 8-11, 2000, Munich Germany

2000-GT-0418

ANALYSIS OF AERODYNAMICALLY INDUCED WHIRLING FORCES IN AXIAL FLOW COMPRESSORS

Z. S. Spakovszky
Gas Turbine Laboratory
Department of Aeronautics and Astronautics
Massachusetts Institute of Technology
Cambridge, MA 02139

ABSTRACT

A new analytical model to predict the aerodynamic forces in axial flow compressors due to asymmetric tip-clearance is introduced. The model captures the effects of tip-clearance induced distortion (i.e. forced shaft whirl), unsteady momentum-induced tangential blade forces and pressure induced forces on the spool. Pressure forces are shown to lag the tip-clearance asymmetry, resulting in a tangential (i.e. whirl-inducing) force due to spool pressure. This force can be of comparable magnitude to the classical Alford force. Prediction and elucidation of the Alford force is also presented.

In particular, a new parameter denoted as the *blade loading indicator* is deduced. This parameter depends only on stage geometry and mean flow and determines the direction of whirl tendency due to tangential blade loading forces in both compressors and turbines.

All findings are suitable for incorporation into an overall dynamic system analysis and integration into existing engine design tools.

NOMENCLATURE

α	absolute inlet swirl angle
β	relative exit swirl angle, Alford parameter
c	chord
D	mean wheel diameter
$f, F, \mathfrak{f}$	loading, force, momentum flux
ϕ	flow coefficient
ε, $\Delta\varepsilon$	tip-clearance / span, shaft offset / span
γ	stagger angle, phase angle
$K_{r\theta}$	cross-coupled stiffness coefficient
l	blade span
λ	rotor blade row inertia
Λ^b	blade loading indicator
$\mathbf{n}$	surface normal
$p, \mathfrak{p}$	static pressure, pressure force
ψ, ψ_h	pressure rise, enthalpy rise
R, ρ	mean wheel radius, density
s	blade pitch
t, T	time, stage torque
θ, θ'	circumferential angle (abs. and rotor frame)
U	mean wheel speed
$v, \mathbf{v}$	absolute velocity (vector)
$w, \mathbf{w}$	relative velocity (vector)
ω, Ω	whirl frequency, rotor frequency
x, y	coordinates in asymmetry frame
x', y'	coordinates in rotor frame
$\tilde{x}, \tilde{y}$	coordinates in absolute frame

INTRODUCTION

Non-uniform engine tip-clearance distributions, due for example to a compressor shaft offset from its casing centerline or whirling in its bearing journal, can induce destabilizing rotordynamic forces. These forces stem from the strong influence of the tip-clearance on the local performance of the compressor. As first reported by Smith (1958), reduced compressor tip-clearance yields increased compressor pressure rise. In the case of an off-

set compressor shaft the blades passing through regions of small tip-clearance will experience higher blade loading and generate more lift than the blades operating in the large tip-clearance region. This results in a net tangential force acting perpendicular to the direction of the shaft offset and is referred to as the aerodynamically induced cross-coupled force.

Early studies conducted by Thomas (1958) and Alford (1965) on axial flow turbines with statically deflected rotors resulted in the postulation of a purely tangential destabilizing reaction force. The so called Alford or Thomas force model is based on a cross-coupled stiffness coefficient $K_{r\theta}$ (tangential force F_θ induced on the rotor per unit radial deflection $\Delta\varepsilon$) of the form

$$K_{r\theta} = \frac{F_\theta}{\Delta\varepsilon} = \frac{\beta\, T}{D\, l}\ , \qquad (1)$$

where T denotes the stage torque, D the mean wheel diameter and l the blade span. The Alford β parameter was originally conceived as the change in thermodynamic efficiency per unit change in normalized clearance. In practice β has become an empirical factor to match computational predictions to experimental data. If β is positive, the net tangential force on the rotor F_θ is in the direction of shaft rotation inducing forward whirl. Similarly, a negative β indicates backward whirl tendency. It is recognized that axial flow turbines tend to generate forward rotor whirl. The early analysis for turbines set the foundation for new research and created an important empirical factor that is considered in the design of modern jet engines and gas turbines.

Several modeling efforts have been undertaken by many researchers (Colding-Jorgensen, 1992; Ehrich, 1993; Yan et al., 1995; Song and Martinez-Sanchez, 1997) to address the issues of whirl-inducing forces in both compressors and turbines. The disparity between the findings and the lack of definitive measurements of cross-coupled excitation forces in axial compressors have led to an experimental and analytical program in the GE Aircraft Engines Low Speed Research Compressor (see Storace et al., 2000; Ehrich et al., 2000). Two important effects, which could not be evaluated in the experimental program and have not yet been modeled in compressors, motivated the work presented here. In the actual case of a whirling shaft (only static shaft deflections could be simulated in the experiment), the unstable rotor would be whirling at the offset radius at the natural frequency of the system. It has been suggested that this whirling might have some significant effect on the value of the Alford β coefficients. Second, non-axisymmetric pressure distributions on the rotor spool were identified as a separate forcing source in turbines and its effects were analyzed by Song and Martinez-Sanchez (1997). It is important to assess the nature and magnitude of non-axisymmetric pressure effects in compressors as well. More specifically the following research questions are of interest and are addressed in this paper:

– How are compressors different from turbines regarding rotor whirl tendency?

– Can one construct a simple analytical model from first principles to determine the whirl tendency in compressors *and* in turbines?

– What drives the destabilizing spool pressure loading and how important is this effect compared to the Alford force?

– How does rotor whirl frequency affect the aerodynamically induced destabilizing forces?

The new model presented here was developed under these thrusts and applied in the GE Aircraft Engines LSRC test program (see Ehrich et al., 2000). In addition a simple, analytical model from first principles is presented which predicts the cross-coupled whirl tendency in compressors and turbines.

MODEL DERIVATION

The new approach consists of two parts: a modified version of an existing 2-dimensional, incompressible tip-clearance compressor stability model reported by Gordon (1999) and an aerodynamically induced force model.

Unsteady Compressor Tip-Clearance Model

Hynes and Greitzer (1987) present a compressor stability model to assess the effect of inlet flow distortion. Based on this conceptual framework Graf et al. (1997) extended this model to account for steady non-axisymmetric tip-clearances. Gordon (1999) further modified this approach to investigate the effect of rotating (unsteady) clearance asymmetries on compressor performance and stability. The unsteady reduced order force model presented in this paper uses a modified version of Gordon's model. The derivation of the compressor model equations is omitted here and a short description of the modified model is given instead.

The overall analysis consists of models of the inlet and exit ducts, the blade rows, the downstream plenum and throttle. The hub-to-tip ratio is assumed high enough to neglect radial variations of the flow quantities. Thus the model is 2-dimensional with axial and circumferential unsteady flow field variations. Effects of viscosity and heat transfer outside of the blade rows are also neglected. The rotor and stator blade rows are modeled as semi-actuator disks with unsteady inertia and loss terms. Unsteady deviation effects are not modeled and the relevant Mach numbers are assumed to be low enough that compressibility effects can be neglected.

The inputs to the model are the compressor geometry, an axisymmetric compressor characteristic and its sensitivity to changes in axisymmetric rotor tip-clearance. Assuming linear

sensitivity, a family of compressor characteristics can be generated which is bounded by the maximum and minimum rotor tip clearance characteristics. In addition any steady or unsteady tip-clearance distribution can be prescribed, e.g. shaft offsets, whirling shafts etc. The compressor operating point is set by the throttle area.

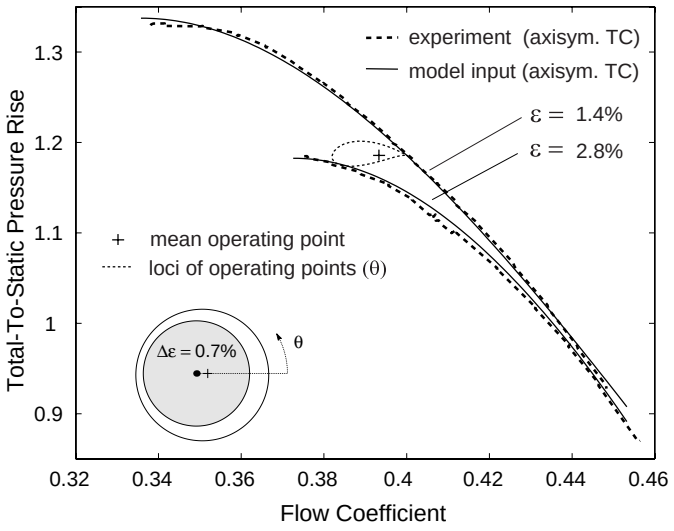

Figure 1. Compressor performance prediction for a steady shaft offset of $\Delta\varepsilon = 0.7\%$ in the four repeating stage compressor reported in Ehrich (1993).

The model assumes that the background flow is steady in the reference frame locked to the (rotating) tip-clearance asymmetry. Hence the steady, non-linear flow field equations are solved in the asymmetry frame (see Figure 3) to obtain the non-uniform background flow. The model outputs the 2-dimensional, non-uniform distribution of flow coefficient, which is steady in the reference frame locked to the tip-clearance asymmetry. In the modified version of the model the entire distorted flow field (axial and tangential velocity and static pressure distributions through the compression system) is reconstructed and transformed back to the absolute frame. This flow field (now unsteady) will be used to determine the aerodynamically induced forces on the rotor.

In this paper, the model will be demonstrated using data (Ehrich, 1993) from a low speed compressor with four repeating stages. Figure 1 depicts the experimentally measured axisymmetric compressor characteristics for ε=1.4% and ε=2.8%, along with the characteristics used as inputs to the model (solid). It also shows the computed mean operating point (+) and the corresponding locus of local operating points around the circumference (lightly dashed) for a steady shaft offset of $\Delta\varepsilon$ = 0.7%. The measurement of mean operating points for a steady shaft offset in the same compressor and comparison to the tip-clearance model predictions is reported in Ehrich et al. (2000).

Aerodynamically Induced Force Model

Once the unsteady, 2-dimensional flow field has been computed as described above, the aerodynamically induced forces can be computed. These forces consist of a spool pressure loading and a tangential force due to asymmetric turning. Simplified expressions for these quantities are derived here, and integrated to get the net forces acting on the rotor.

The spool pressure loading in the rotor frame is readily obtained from the flow field solution. Since the compressor blade rows have been modeled as semi-actuator disks, only the static pressure distribution between the blade rows can be directly computed. The unsteady spool pressure loading $p_{\text{spool}}(\theta',t)$ (where $\theta' = (\theta - \Omega t)$ is the tangential coordinate in the rotor frame) is estimated by averaging the static pressures upstream and downstream of the rotor:

$$p_{\text{spool}}(\theta',t) = \frac{p_1(\theta',t) + p_2(\theta',t)}{2} \,. \tag{2}$$

This approach assumes that the blade pitch is much smaller than the wavelength of the circumferential pressure distribution and makes use of the high hub-to-tip ratio assumption.

To determine the local, unsteady tangential blade loading $f_\theta(\theta',t)$, an *unsteady* control volume analysis is conducted locally in the rotor frame. The advantage of this approach is that any unsteady flow regime (whirling shaft, rotating stall etc.) can be considered. A control volume is defined in the rotor frame bounding one blade along the steady streamlines as sketched in Figure 2, where the relative velocity vectors are labeled with **w**. The blade pitch, blade span, blade chord, mean wheel radius and the stagger angle are denoted by s, l, c, R and γ respectively. Generally the vector momentum equation in integral form is written for inviscid flows as

$$\begin{aligned} \frac{\partial}{\partial t}\oint_V \rho\,\mathbf{v}\,dV + \oint_{\partial V}(\rho\,\mathbf{v}\cdot\mathbf{n}\,dS)\mathbf{v} = \\ -\oint_{\partial V} p\,\mathbf{n}\,dS + \oint_V \rho\,\mathbf{f}_\text{b}\,dV \,, \end{aligned} \tag{3}$$

where **v** is the velocity field vector, p the static pressure field and $\mathbf{f}_\text{b}$ the elemental body force vector per unit mass. Assuming incompressible flow through a constant height annulus, applying Equation (3) to the control volume in Figure 2 in the tangential direction and replacing the body force integral by the *total* blade loading $F_{l\theta}$ of opposite sign (the body force acting on the fluid is equal to the negative of the fluid force on the body: $\mathbf{f}_\text{b} = -\mathbf{F}_{l\theta}$)

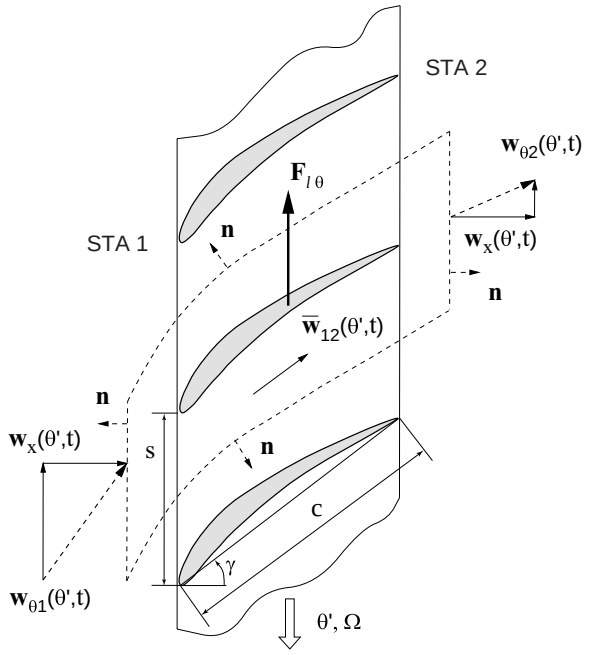

Figure 2. Unsteady momentum control volume analysis locked to rotor frame.

yields

$$-\rho\, s\, l \cos\gamma\, c\, \frac{\partial}{\partial t}\overline{w_{\theta}}_{12} + \rho\, s\, l \cdot w_x \cdot (w_{\theta 1} - w_{\theta 2}) + \Delta \mathfrak{f}_{ss} = \Delta \mathfrak{p}_{ss} + F_{l\theta}\,. \tag{4}$$

The contributions of the net momentum flux and net pressure force across the stream-wise surface boundaries are denoted by $\Delta\mathfrak{f}_{ss}$ and $\Delta\mathfrak{p}_{ss}$ respectively. Note that the only pressure terms arise from the stream-wise surface boundaries since the pitch-wise surface normal **n** is perpendicular to the tangential direction θ'. It is assumed for the unsteady term that the velocity inside the control volume is equal to the average of the velocities at stations 1 and 2 [1]. The projection of this average velocity in the θ direction is denoted by $\overline{w_{\theta}}_{12}$.

The obtained expression is fairly complicated and needs to be simplified. Intuitively one can argue that if the wavelength of the flow non-uniformity is large compared to the blade pitch *s*, then $\Delta\mathfrak{f}_{ss}$ and $\Delta\mathfrak{p}_{ss}$ across the stream-wise surfaces should vanish in magnitude compared to the unsteady and the tangential momentum flux terms. In fact, if the control volume width set by blade pitch *s* is taken to the limit $R \cdot d\theta$, it can be shown that the stream-wise surface terms are negligible to first order. The *local* (per unit circumferential angle), unsteady, tangential blade loading f_θ can then be written as

$$f_\theta(\theta',t) = \rho\, R\, l \cdot w_x \cdot (w_{\theta 1} - w_{\theta 2}) - \frac{\rho\, R\, l \cos\gamma\, c}{2}\, \frac{\partial}{\partial t}\{w_{\theta 1} + w_{\theta 2}\}\,. \tag{5}$$

The next step is to integrate the spool pressure loading and tangential blade loading distributions defined in Equations (2) and (5) around the circumference. This is done in the rotor reference frame (x',y') shown in Figure 3 to obtain the unsteady forces on the rotor:

$$f^s_{x'}(t) = -\int_0^{2\pi} p_{\text{spool}}(\theta',t) \cdot \cos(\theta') \cdot c_{\text{sp}}\, R \cdot d\theta'$$

$$f^s_{y'}(t) = -\int_0^{2\pi} p_{\text{spool}}(\theta',t) \cdot \sin(\theta') \cdot c_{\text{sp}}\, R \cdot d\theta' \tag{6}$$

$$f^b_{x'}(t) = +\int_0^{2\pi} f_\theta(\theta',t) \cdot \sin(\theta') \cdot d\theta'$$

$$f^b_{y'}(t) = -\int_0^{2\pi} f_\theta(\theta',t) \cdot \cos(\theta') \cdot d\theta'$$

where the superscripts ^{s} and ^{b} denote *spool* loading and *blade* loading respectively. The spool pressure load acts on the spool surface of axial length c_{sp} which includes the inter-blade row gaps upstream and downstream of the rotor. Finally, these unsteady forces are transformed back to the reference frame locked to the tip-clearance asymmetry using the transformation given in Equation (7) to get the aerodynamically induced forces F^s_x, F^s_y, F^b_x and F^b_y.

$$\begin{bmatrix} F_x \\ F_y \end{bmatrix} = \begin{bmatrix} \cos((\Omega-\omega)\,t) & -\sin((\Omega-\omega)\,t) \\ \sin((\Omega-\omega)\,t) & \cos((\Omega-\omega)\,t) \end{bmatrix} \cdot \begin{bmatrix} f_{x'}(t) \\ f_{y'}(t) \end{bmatrix}\,. \tag{7}$$

Note that, since the model assumed steady flow in the reference frame of rotating tip-clearances, the aerodynamically induced forces are steady in the asymmetry frame.

The magnitude and direction of the four aerodynamically induced rotor forces F^s_x, F^s_y, F^b_x and F^b_y are discussed next. The main focus will be on the sign of F^b_y, F^s_y and their sum, since they determine the tendency of shaft whirl. Two parameters will be used in the analysis, the Alford β parameter (non-dimensional F^b_y) and a new parameter denoted as the spool loading parameter β_{spool} (non-dimensional F^s_y).

[1] Using this particular tip-clearance compressor model the flow field *inside* the blade rows cannot be reconstructed (actuator disk approach).

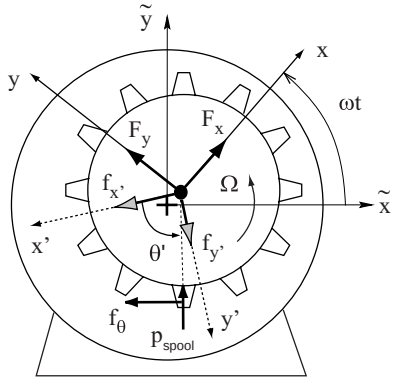

Figure 3. Definition of reference frames: rotor frame (x',y'), rotating asymmetry frame (x,y) and absolute frame $(\tilde{x},\tilde{y})$.

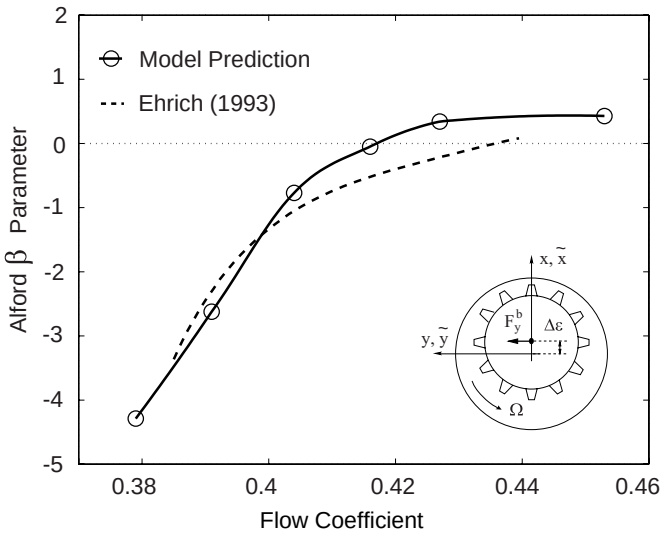

Figure 4. Alford β parameter for four stage compressor reported in Ehrich (1993) and model prediction.

ANALYSIS AND MODELING RESULTS

The model is implemented in an example analysis for the second stage of the four repeating stage axial compressor reported in Ehrich (1993).

Importance of the Alford β Parameter

In the case of a steady shaft offset the tip-clearance asymmetry frame is identical to the absolute frame. The aerodynamic force model is implemented for the example compressor with a shaft offset of $\Delta\varepsilon = 0.7\%$. To analyze the destabilizing effect of a net tangential blade loading only F_y^b is considered here. The Alford β parameter (Equation (1)) is computed using the same mean stage torque T as in Ehrich (1993) in order to compare the model predictions to the experimentally-driven results of Ehrich. The direction of whirl depends on the direction of the net tangential force F_y^b with respect to shaft rotation. If F_y^b is positive (in the direction of rotation) β is positive and the rotor will tend to forward whirl. Similarly, a negative β indicates backward whirl tendency. The Alford β parameter is plotted for different flow coefficients in Figure 4 (solid line). The magnitude of the Alford β parameter and the dependence of the whirl direction on the flow coefficient agrees well with the experimentally-based predictions by Ehrich (1993) (dashed line). For low flow coefficients a strong backward whirl tendency is predicted whereas forward whirl is induced for high flow coefficients. It should be mentioned that three-dimensional phenomena such as stator hub clearance and seal leakage effects can alter the Alford β parameter and are not accounted for in the two-dimensional approach. A comparison of the modeling results to experimental blade force data obtained in the GE Aircraft Engines LSRC facility and a discussion of the stator clearance and seal leakage effects are given in Ehrich et al. (2000).

The 2-dimensional unsteady modeling approach seems to capture the observed compressor phenomena well. The following questions arise from the result above: what determines the direction of whirl tendency in compressors and how do compressors differ from turbines in this regard?

Blade Loading Indicator Parameter

In order to assess the difference between the whirl tendency in compressors and the whirl tendency in turbines, one would like to construct a general, simple analytical model from first principles. Simplifying Equation (5) by neglecting unsteady effects and again assuming constant axial velocity through the stage, the tangential momentum balance can be written for both compressors and turbines as shown in Figure 5a and b, where f_θ^{comp} and

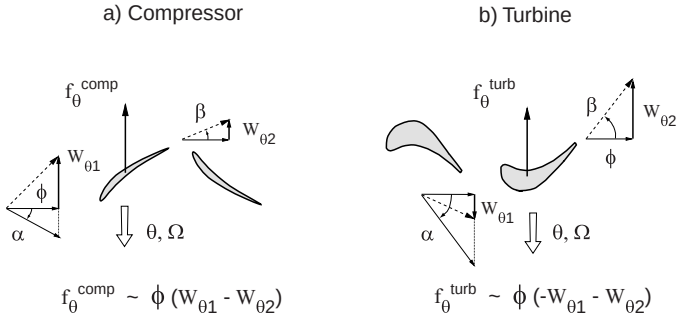

Figure 5. Simplified blade loading analysis for compressors and turbines.

f_θ^{turb} denote compressor and turbine tangential blade loading, ϕ is the flow coefficient and $W = w/U$ is the non-dimensional relative velocity. Using kinematic relations and the velocity triangles the tangential blade loading can be written in general as

$$f_\theta \sim \phi \cdot [1 - (\tan\alpha + \tan\beta) \cdot \phi] = \phi \cdot \psi_h^I . \quad (8)$$

Note that f_θ points in the negative θ direction in Figure 5. This expression holds for both compressors and turbines where ψ_h^I is the ideal static enthalpy rise for compressors or the ideal static enthalpy drop for turbines, α is the absolute inlet swirl angle and β denotes the relative exit swirl angle. Since only variations in tangential blade loading distribution contribute to the net tangential rotor force F_y^b, Equation (8) can be expanded to first order and written as

$$\delta f_\theta \sim -[2\,(\tan\alpha + \tan\beta) \cdot \bar{\phi} - 1] \cdot \delta\phi . \quad (9)$$

Let the bracketed expression be denoted as the *blade loading indicator* Λ^b which only depends on the stage geometry and the mean value of the flow coefficient $\bar{\phi}$. If the tip-clearance is increased the blockage increases and yields a decrease in flow coefficient ($\delta\varepsilon \sim -\delta\phi$). Combining this with Equation (9) the following simple relation holds between the tip-clearance distribution and the distribution of the local tangential blade loading:

$$\delta f_\theta \sim \Lambda^b \cdot \delta\varepsilon . \quad (10)$$

Let us assume that the variation in flow coefficient is purely sinusoidal and flow inertia effects are neglected. If Λ^b is positive δf_θ is in phase with the tip-clearance distribution and integration around the annulus yields a positive net tangential blade loading F_y^b (in the direction of rotation). The opposite holds for a negative blade loading indicator inducing F_y^b in the negative direction as sketched in Figure 6 at the top. Hence the blade loading indicator is conjectured to determine the whirl direction for compressors and turbines[2].

This simple model is applied to the four stage compressor reported in Ehrich (1993). The inlet and exit swirl angles are known at mid span and assumed to be constant over the compressor operating range yielding $\tan\alpha + \tan\beta = 1.16$. Setting the blade loading indicator Λ^b to zero one can solve for the mean flow coefficient $\bar{\phi}$ for which the net tangential force should vanish. For this particular compressor if $\bar{\phi} = 0.431$ the net tangential rotor force is zero, if $\bar{\phi} > 0.431$ then Λ^b is positive inducing forward whirl and if $\bar{\phi} < 0.431$ the compressor tends to backward whirl due to a negative blade loading indicator Λ^b. This situation is sketched in Figure 6 together with the ideal compressor characteristic $\bar{\psi}_h^I$. Comparison of this result to the experimentally

[2]This analysis is limited to the sign of the Alford β only and does not include the effect of spool pressure loading.

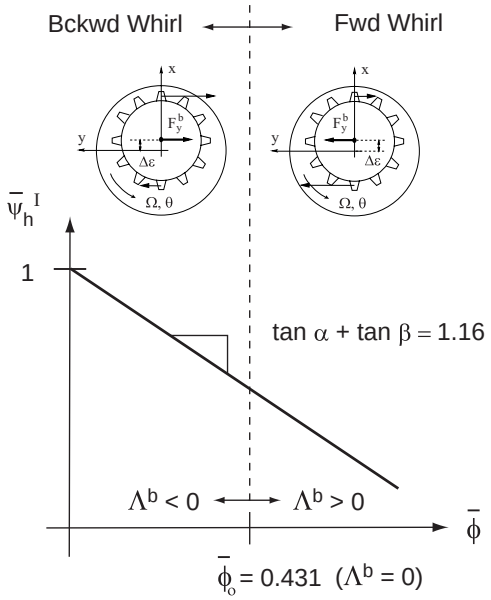

Figure 6. Simplified whirl analysis of four stage compressor.

based Alford β predictions by Ehrich (1993) in Figure 4 shows that the β curve crosses zero at a flow coefficient of 0.435. This agrees well with the simple model result of $\bar{\phi} = 0.431$ and the predictions of whirl direction tendency. In order to give more generality to the assessment, two other compressors reported in Ehrich (1993) are analyzed. The predictions by the simple, first principles approach and experimentally based results by Ehrich (1993) are summarized for all three compressors in Table 1.

Method	Compressor I	Compressor II	Compressor III
$\Lambda^b = 0$	$\bar{\phi}_o = 0.464$	$\bar{\phi}_o = 0.506$	$\bar{\phi}_o = 0.431$
Ehrich	$\bar{\phi}_o = 0.457$	$\bar{\phi}_o = 0.490$	$\bar{\phi}_o = 0.435$

Table 1. Experimentally based predictions (Ehrich, 1993) and Λ^b approach for three axial flow compressors reported in Ehrich (1993): backward whirl tendency for $\bar{\phi} < \bar{\phi}_o$, forward whirl tendency for $\bar{\phi} > \bar{\phi}_o$.

The simple model can also be applied to turbines. Turbines inherently exhibit much higher flow turning than compressors, especially if they are of impulse type with a degree of reaction close to zero. Hence the absolute inlet and relative exit swirl angles will be much higher than in a compressor rotor. Therefore the blade loading indicator Λ^b is always positive and its sign is independent of the mean flow coefficient unless $\bar{\phi}$ is very small or the degree of reaction is relatively high (less turning). This leads to the conjecture that, in turbines, the net tangential blade

loading induces forward whirl over the entire operating range. This is in agreement with Alford's hypothesis and observations reported in literature.

Effects of Spool Pressure Loading

Non-axisymmetric pressure distributions on the rotor spool were identified as a separate forcing source in turbines and its effects were analyzed by Song and Martinez-Sanchez (1997). It is suggested that this effect is also important in compressors and its nature and magnitude are assessed in this section.

To quantify the destabilizing effect of spool pressure loading, a parameter similar to the Alford β coefficient is defined:

$$\beta_{\text{spool}} = \frac{F_y^s \, D \, l}{T \, \Delta\varepsilon} \, . \tag{11}$$

The β_{spool} parameter is computed for different flow coefficients and plotted in Figure 7. Forward whirl ($\beta_{\text{spool}} > 0$) is induced, with a maximum value of β_{spool} near compressor stall. This is mostly due to the fact that the flow field is more distorted for flow coefficients less than 0.41 (the family of compressor characteristics are further apart at low flows in Figure 1). The magnitude

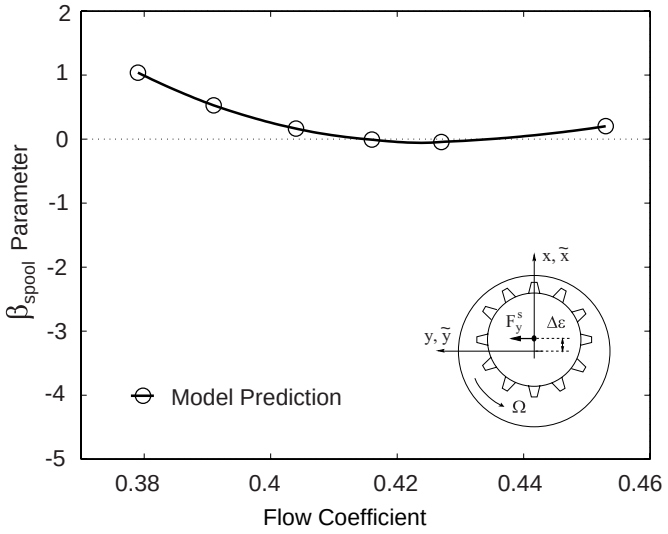

Figure 7. Spool loading parameter β_{spool} for four repeating stage compressor reported in Ehrich (1993).

of β_{spool} is about half the magnitude of the Alford β parameter for low flow coefficients. Note that the forward whirl induced by spool pressure loading mitigates the backward whirl tendency due to the net tangential blade loading (Figure 4). The nature of the forward whirl tendency due to spool pressure effects is discussed next.

First let us consider a family of axisymmetric tip-clearance compressor characteristics with no curvature and neglect unsteady losses and flow inertia effects in the blade rows and ducts. In this case the flow instantaneously responds to the distortion induced by the asymmetric tip-clearance. Regions with tight tip-clearance yield high total-to-static pressure rise, less blockage and therefore a higher flow coefficient. Conserving total pressure in the upstream duct (potential flow) and matching the uniform pressure distribution at the compressor exit yields a lower spool pressure in the tight tip-clearance region. The opposite holds for regions of large tip-clearance. The variation in total-to-static pressure rise $\delta\psi_{ts}$, the variation in flow coefficient $\delta\phi$ and the variation in non-dimensional spool pressure $\delta p_{\text{spool}}/\rho U^2$ are plotted in Figure 8 as dashed lines for the given shaft offset (the tip-clearance distribution is shown as the dotted line in the top plot). Evaluation of the first two integrals in Equation (6) and

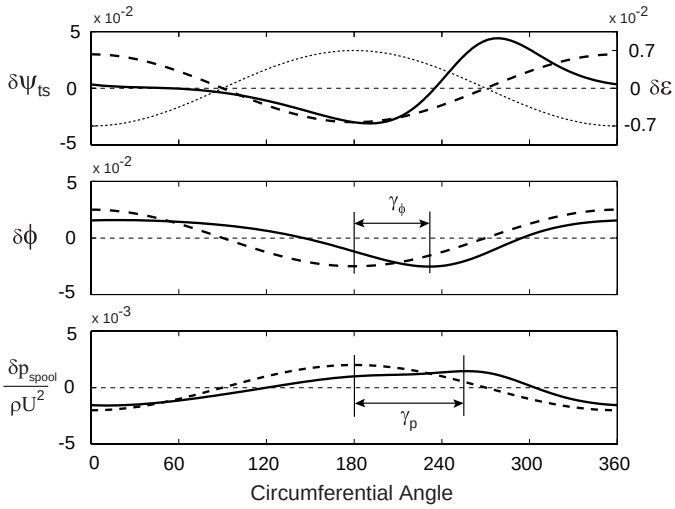

Figure 8. Compressor flow field with inertia effects included (solid) and inertia effects neglected (dashed) for a given tip-clearance distribution $\delta\varepsilon$ (dotted).

transformation to the frame of the shaft offset using Equation (7) yields $F_x^s > 0$ and $F_y^s = 0$ for this sinusoidal spool pressure distribution. In other words, the aerodynamically induced rotor force due to spool loading is a purely radial destabilizing force, as sketched in Figure 9a. The purely sinusoidal spool pressure loading distribution does not induce whirl since the aerodynamic rotor force has no tangential component ($F_y^s = 0$).

Now let us consider the family of compressor characteristics shown in Figure 1 and assume that unsteady losses and unsteady flow inertia effects are present. The total-to-static pressure rise distribution $\delta\psi_{ts}$ is now distorted due to the curvature of the compressor characteristics as depicted in the top plot of Figure 8 (solid line). A part of the compressor pressure rise is now devoted to acceleration of the fluid in the blade row passages. As-

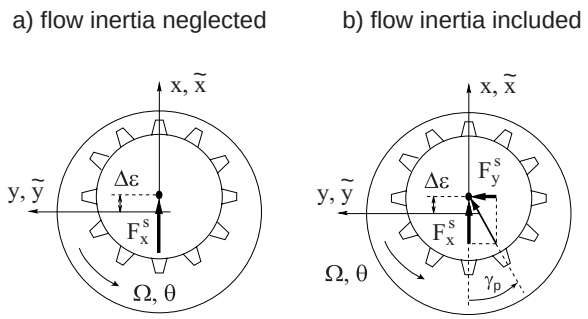

Figure 9. Effect of flow inertia on rotor forces due to spool pressure loading.

suming quasi-steady flow and no exit swirl it can be shown that the following pressure balance across the compressor must hold:

$$\frac{p^{\mathrm{dn}} - p_t^{\mathrm{up}}}{\rho\, U^2} = \psi_{ts} - \lambda \cdot \frac{\partial \phi}{\partial \theta}\,, \tag{12}$$

where λ denotes the non-dimensional fluid inertia in the rotor blade rows (Moore and Greitzer, 1986)

$$\lambda = \sum_{\mathrm{rotors}} \frac{\phi/R}{\cos^2 \gamma}\,. \tag{13}$$

In steady flow the compressor upstream total pressure p_t^{up} and compressor downstream static pressure p^{dn} are uniform, so circumferential variations in ψ_{ts} must be directly balanced by variations in the gradient of flow coefficient

$$0 = \delta\psi_{ts} - \lambda \cdot \frac{\partial \delta\phi}{\partial \theta}\,. \tag{14}$$

This explains why the flow coefficient variation lags the clearance distribution in Figure 8. Including flow inertia in the compressor model results in a relative phase shift in the flow coefficient and spool pressure distributions, denoted γ_ϕ and γ_p in Figure 8. Due to this positive phase shift, the spool pressure loading now also yields a force component in the tangential direction F_y^s and induces forward whirl as shown in Figure 9b.

Effects of Forced Shaft Whirl

In the case of a whirling shaft, the rotor would be whirling at the offset radius at the natural frequency of the system. It is therefore important to assess the effects of this whirling on the β parameters.

The following parameter study is conducted to assess the effects of forced shaft whirl on the destabilizing rotor forces. The whirl frequency ω is varied from synchronous backward whirl ($\omega = -\Omega$) to synchronous forward whirl ($\omega = \Omega$) for a shaft offset of $\Delta\varepsilon = 0.7\%$. The aerodynamically induced forces acting in the rotating asymmetry frame are computed using Equations (6) and (7). In order to examine the whirl tendency due to unbalanced blade and spool loading effects, the Alford β parameter and the spool loading parameter β_{spool} are determined. Figure 10 depicts the β parameters for different flow coefficients and non-dimensional whirl frequencies ω/Ω. The tip-clearance

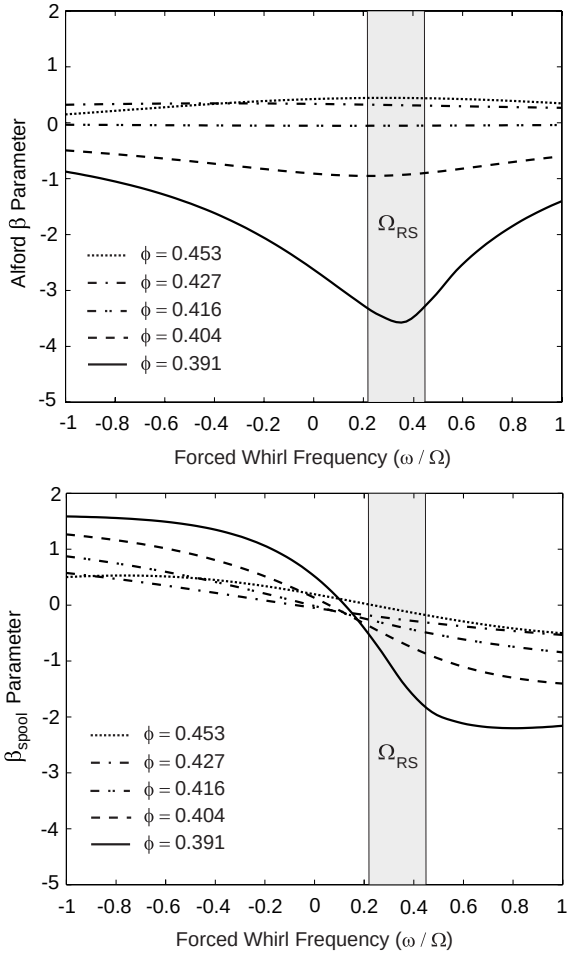

Figure 10. Alford β parameter and spool loading parameter β_{spool} for forced rotor whirl.

compressor model can also be used to determine compressor stability. Due to the flow distortion, which is affected by the shaft whirl, the rotating stall frequency varies slightly with the forced whirl frequency. For the four stage compressor discussed here, rotating stall is predicted to occur between 22% and 46% of rotor frequency. This rotating stall frequency range is indicated by

Ω_{RS}.

Notice that for low flow coefficients the Alford β parameter is amplified and the spool loading β_{spool} changes sign close to zero forced whirl frequency. A detailed analysis of the flow field shows that the rotating tip-clearance asymmetry induces an enhanced distortion of the flow near rotating stall. Consider an observer sitting on the rotating asymmetry frame at the location of the smallest tip-clearance. The observer will then perceive a steady, non-uniform flow field which will have a certain orientation relative to the observer's location. The phase and the magnitude of the fundamental wave form (a single lobed sinusoid indicated by subscript $_1$) of the flow coefficient and the non-dimensional spool pressure are analyzed for different forced whirl frequencies. The results for a compressor operating point close to stall are shown in Figure 11 and the rotating stall frequency range is again indicated by Ω_{RS}.

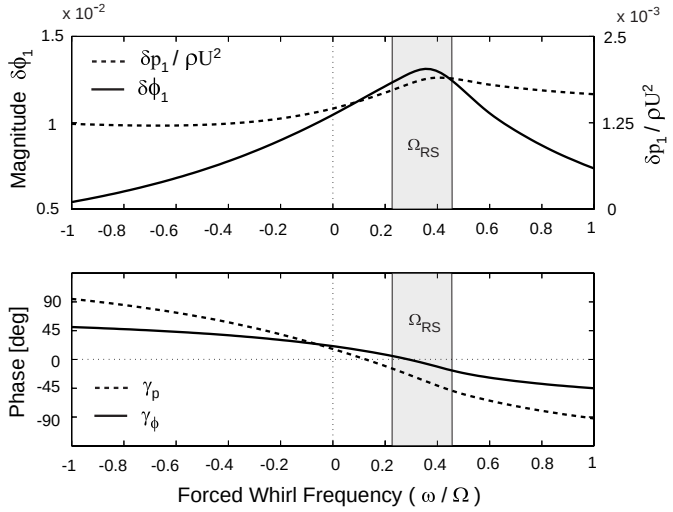

Figure 11. Magnitude and phase of fundamental wave form of flow coefficient (solid) and non-dimensional spool pressure (dash) for $\phi = 0.391$.

If shaft motion occurs at negative whirl frequencies the flow field lags the clearance asymmetry and the relative phase between the clearance asymmetry and the spool pressure distribution γ_p is positive. This translates to a spool loading induced forward whirl as described in Figure 9. The opposite holds for positive whirl frequencies higher than 0.1 and yields backward whirling forces, as shown in the bottom plot of Figure 10. Similar arguments hold for the blade loading distribution since the relative phase between the net tangential blade loading F_y^b and the rotating clearance asymmetry can be related to the phase of the flow coefficient (see Equation (5)). Notice that γ_ϕ never exceeds $\pm 90^o$ so that F_y^b does not change sign. This yields a whirl frequency independence of the sign of the Alford β parameter as shown in the top plot of Figure 10. The enhanced flow field distortion and the zero phase γ_ϕ near the rotating stall frequency (see Figure 11) are felt in the net tangential blade loading and reflected in an amplification of β near Ω_{RS}.

It is important to note the following results from Figure 10. (1) The spool loading parameter β_{spool} acts in the direction against whirl for both large positive and negative forced whirl frequencies. (2) β_{spool} is of comparable magnitude to the Alford β. (3) β_{spool} opposes the effects of the Alford β for two cases: for negative whirl frequencies and low flow coefficients and for positive whirl frequencies and high flow coefficients. (4) The net effect of β_{spool} and the Alford β yields backward whirl for forced whirl frequencies ranging from -0.5 to +1. To the author's knowledge no rotor whirl experiment has been reported in literature in order to compare the modeling results to data. Spakovszky et al. (2000) report a feasibility study of a magnetic bearing servo actuator for a high-speed compressor stall control experiment. The described experiment could be used to actively whirl and precess the compressor shaft to investigate rotordynamic-aerodynamic coupling effects.

Note also that the frequency coincidence between enhanced whirl tendency and rotating stall leads to the conjecture that in an engine, where the rotordynamics and compressor aerodynamics form one dynamic system, shaft whirl can interact and resonate with flow instability patterns such as rotating stall. The current uncoupled modeling results are an important piece of an overall dynamic system analysis since they separate the basic effects of whirl inducing forces. A non-linear, coupled system analysis is suggested to investigate the dynamic behavior of the compressor-rotor system. Current research on rotordynamic-aerodynamic interaction in axial compression systems is reported by Al-Nahwi (2000).

CONCLUSIONS AND SUMMARY

This paper reports a new unsteady low order model to predict aerodynamically induced whirling forces in axial flow compressors. The model consists of two parts: a tip-clearance induced distortion model and an aerodynamically induced force model. The distortion model predicts the flow response to given (rotating) tip-clearance asymmetries. The force model then uses this distorted unsteady flow field to deduce the forces on the rotor. The force model is not limited to this particular compressor model; any prediction of the compressor flow field can be used (i.e. CFD, experimental data etc.). The model computes destabilizing rotor forces due to non-uniform tangential blade loading and non-uniform spool pressure loading effects for steadily deflected and whirling shafts.

The model is implemented in an example analysis for the four repeating stage axial compressor reported in Ehrich (1993). A steady shaft offset of $\Delta\varepsilon = 0.7\%$ tip-clearance over span is considered first and the computed Alford β parameter is in good agreement with the results reported in Ehrich (1993).

In addition, a simple model from first principles is presented. This analytical approach introduces a simple parameter denoted as the *blade loading indicator*. The blade loading indicator depends only on the stage geometry and the mean flow coefficient and determines the direction of whirl tendency due to tangential blade loading forces in both compressors and turbines.

A spool loading parameter β_{spool}, analogous to the Alford β parameter, is introduced and predicts forward whirl for steady shaft offsets. The effect of flow inertia on the spool pressure loading is investigated and the modeling results show that the flow field lags the clearance distribution due to the fluid inertia. This phase shift induces destabilizing rotor forces, due to spool pressure loading effects, which add to the forces predicted by Alford.

Forced shaft whirl is simulated to assess the effects of shaft motion on the destabilizing rotor forces. The β_{spool} parameter acts in the direction against whirl and is of comparable magnitude to the Alford β. It opposes the effects of the Alford β for negative whirl frequencies and low flow coefficients and for positive whirl frequencies and high flow coefficients. Also, the frequency coincidence between shaft whirl and rotating stall suggests non-linear coupling effects between the aerodynamics and the rotordynamics.

An important element in the design of rotordynamically stable jet engines is the accurate prediction of the aerodynamically induced forces. The reported results are compared to experimental blade force data obtained from the GE Aircraft Engines LSRC test facility in Ehrich et al. (2000). The presented aerodynamically induced force model forms an important basis for an overall dynamic system analysis and is suggested as an integral part of engine design tools.

ACKNOWLEDGMENTS

The author would like to thank A. Al-Nahwi and Dr. F. Ehrich for the very useful comments and insightful discussions. This research was conducted under NASA grant NAG3-2052.

REFERENCES

Al-Nahwi A., 2000. "*Rotordynamic-Aerodynamic Interaction in Axial Compression Systems*." Ph.D. thesis in preparation, Dept. of Mechanical Engineering, MIT.

Alford J., 1965. "Protecting Turbomachinery from Self-Excited Rotor Whirl." *ASME J. of Engineering for Power*, vol. 87 pp. 333–344.

Colding-Jorgensen J., 1992. "Prediction of Rotor Dynamic Destabilizing Forces in Axial Flow Compressors." *ASME J. of Fluids Engineering*, vol. 114 pp. 621–625.

Ehrich F., 1993. "Rotor Whirl Forces Induced by the Tip Clearance Effect in Axial Flow Compressors." *ASME J. of Vibration and Acoustics*, vol. 115 pp. 509–515.

Ehrich F., Spakovszky Z., Martinez-Sanchez M., Song S., Wisler D., Storace A., Shin H.W., and Beacher B., 2000. "Unsteady Flow and Whirl Inducing Forces in Axial-Flow Compressors; Part II - Analysis." In *ASME Turbo Expo, Munich, Germany*.

Gordon K., 1999. *Three-Dimensional Rotating Stall Inception and Effects of Rotating Tip Clearance Asymmetry in Axial Compressors*. Ph.D. thesis, Department of Aeronautics and Astronautics, MIT.

Graf M., Wong T., Greitzer E., Marble F., Tan C., Shin H.W., and Wisler D., 1997. "Effects of Non-Axisymmetric Tip Clearance on Axial Compressor Performance and Stability." In *ASME Turbo Expo, Orlando, FL, Paper 97-GT-406*.

Hynes T. and Greitzer E., 1987. "A Method for Assessing Effects of Circumferential Flow Distortion on Compressor Stability." *ASME J. of Turbomachinary*, vol. 109 pp. 371–379.

Moore F. and Greitzer E., 1986. "A Theory of Post-Stall Transients in Axial Compressors: Part I — Development of the Equations." *ASME J. of Engineering for Gas Turbines and Power*, vol. 108 pp. 68–76.

Smith L., 1958. "The Effect of Tip Clearance on the Peak Pressure Rise of Axial-Flow Fans and Compressors." *ASME Symposium on Stall* pp. 149–152.

Song S. and Martinez-Sanchez M., 1997. "Rotordynamic Forces Due to Turbine Tip Leakage: Part I - Blade Scale Effects." *ASME J. of Turbomachinary*, vol. 119 pp. 695–703.

Spakovszky Z., Paduano J., Larsonneur R., Traxler A., and Bright M., 2000. "Tip-Clearance Actuation with Magnetic Bearings for High-Speed Compressor Stall Control." In *ASME Turbo Expo, Munich, Germany*.

Storace A., Wisler D., Shin H.W., Beacher B., Ehrich F., Spakovszky Z., Martinez-Sanchez M., and Song S., 2000. "Unsteady Flow and Whirl Inducing Forces in Axial-Flow Compressors; Part I - Experiment." In *ASME Turbo Expo, Munich, Germany*.

Thomas H., 1958. "Unstable Natural Vibration of Turbine Rotors Induced by the Clearance Flow in Glands and Blading." *Bull. de l'A.I.M*, vol. 71, no. 11/12 pp. 1039–1063.

Yan L., Hong J., Li Q., Zhu Z., and Zhao F., 1995. "Blade Tip Destabilizing Force and Instability Analysis for Axial Rotors of Compressors." Beijing University of Aeronautics and Astronautics.